The Chemist
Journal of the American Institute of Chemists

Structural and Optical Properties of Zinc Oxide Nanorods Prepared by Aqueous Solution Route

David Devraj Kumar[a], Prabitha B. Nair[b], Justinvictor V. B.[b], P. V. Thomas[b, *]

[a] STEM Education Lab, College of Education, Florida Atlantic University, 3200 College Ave, Davie, FL 33314, USA.

[b] Thin Film Lab, Research Center, Department of Physics, Mar Ivanios College, Thiruvananthapuram-695015, India.

*(*Email: thomaspv_15@yahoo.com)*

Abstract: Preparation of ZnO nanorods was successfully carried out by a simple cost-effective precipitation from an aqueous solution route at a low temperature (353K). Detailed structural and optical characterizations were performed using x-ray diffraction (XRD), scanning electron microscope (SEM), ultraviolet-visible (UV-Visible) spectrophotometry, and Photo Luminescence (PL) spectroscopy. Results revealed the formation of high quality ZnO nanorods in a wurtzite hexagonal crystal phase. The electronic energy state transition spectrum revealed an optical band gap of 3.37 eV. Measured PL intensities due to exciton emission and deep level emissions indicated the quality of the nanorods prepared by this method. PL spectra showed an intense blue emission by the ZnO rods, which increased with a rise in calcination temperature.

Key Words: Zinc oxide, nanorods, band gap, photoluminescence.

INTRODUCTION

Zinc oxide is a II-VI semiconducting material having a wurtzite hexagonal structure with lattice parameters a=3.2501Å and c=5.2066 Å [1]. It is a unique material that possesses attractive electronic properties, such as wide band gap (3.37eV) and large exciton energy (60 meV) [2], in addition to semiconducting, piezoelectric and pyroelectric properties. The strong exciton binding energy indicates efficient exciton emission in the UV region. This property makes it a promising photonic material in the blue-UV region [3]. ZnO nanomaterials in the form of nanowires and nanorods are important due to their applications in tunable electronic and optoelectronic devices [4].

Several methods have been proposed for the preparation of ZnO nanorods, such as hydrothermal and thermal decomposition methods, sol gel synthesis, chemical vapor deposition, spray pyrolysis, and precipitation method [5-10]. Control of the particle shape is a major concern for nanostructured material synthesis because electrical and optical properties of nanomaterials depend sensitively on both size and shape of the particle. Therefore, it is desirable to prepare nanomaterials of controllable shape and size by a simple approach. For zinc oxide particles, various shapes, including nanorods [7,11-14], whiskers [15,16], and nanowires [17], have been successfully prepared. A simple chemical route to the preparation of ZnO nanorods has been reported where thermal decomposition of $ZnC_2O_4.2H_2O$ resulted from the reaction of $Zn(CH_3COO)_2.2H_2O$ and $H_2C_2O_4.2H_2O$ with surfactant phenyl ether and NaCl flux [14]. Hydrothermal preparations of ZnO nanorods from aqueous $Zn(NO_3)_2$ and KOH at 673 K with a simple apparatus and without organic feed reagents have yielded ZnO nanorods in average 230nm in length and 38nm in width [13]. But many of the synthesis methods reported require complex experimental conditions, substrates, and sophisticated instruments [7,18]. Also, most of the methods produce nanorods or tubes in small quantities at high cost. Therefore, a simple preparation route to ZnO nanorods is of great importance. See, for example, a template-free aqueous route to the preparation of ZnO nanorods that was reported showing useful optical properties by PL spectroscopy [19]. In the present work, a similarly simple

© The AIC 2016. All rights reserved.

aqueous solution route for the preparation of ZnO nanorods at low temperatures and at normal conditions of pressure, without using any templates or surfactants, is presented. The quality of the nanorods is high in terms of their crystallinity and optical properties.

EXPERIMENT

ZnO nanorods were prepared by precipitation from an aqueous solution. Analytical-grade zinc nitrate hexahydrate [$Zn(NO_3)_2.6H_2O$] and sodium hydroxide (NaOH) were used without further purification. In a typical synthesis for the growth of ZnO nanorods, 3g of $Zn(NO_3)_2.6H_2O$ was dissolved in 200 ml of distilled water and stirred for 30 minutes. Then, 40 ml, 0.1M NaOH was added slowly, drop wise, under vigorous stirring using a magnetic stirrer until the slow precipitation of ZnO was completed. During this process, the temperature of the $Zn(NO_3)_2.6H_2O$ solution was kept constant at 353 K. It was then kept at 353 K in an electric furnace for 3 hours in ambient atmospheric conditions. The precipitate was filtered and washed several times with distilled water and ethanol. The final product was air-dried at room temperature and characterized as follows.

The structural properties of the prepared ZnO nanoparticles were studied using a PAN ANALYTICAL™ X-ray diffractometer. A Cu target (Cu Kα radiation, λ=0.15418 nm) was used as the X-ray source. Data was collected in the range 2θ = 20-70°, at a scanning speed of 4° per minute. UV-VIS spectrophotometry was used to record the reflectance spectra of the sample. The spectra were recorded in reflectance mode using a JASCO spectrophotometer, model V-550™, equipped with an integrating sphere attachment. $BaSO_4$ was used as the reference sample. Photoluminescence (PL) spectra were recorded at room temperature using a Perkin Elmer LS55™ spectrophotometer. The surface morphology and size of the nanorods were determined using a Scanning Electron Microscopy (CARL ZEISS EVO50) ™. The samples were calcined at 523K and 673K in air and the effect of calcination on the PL spectra of the samples was investigated.

RESULTS & DISCUSSION

Surface morphology - SEM

Figure 1 shows the surface morphology of the prepared nanoparticles in the form of nanorods. The grown nanorods are solid and straight with non-uniform widths and lengths. The average length and diameter of a typical rod is 300 nm and 200 nm, respectively.

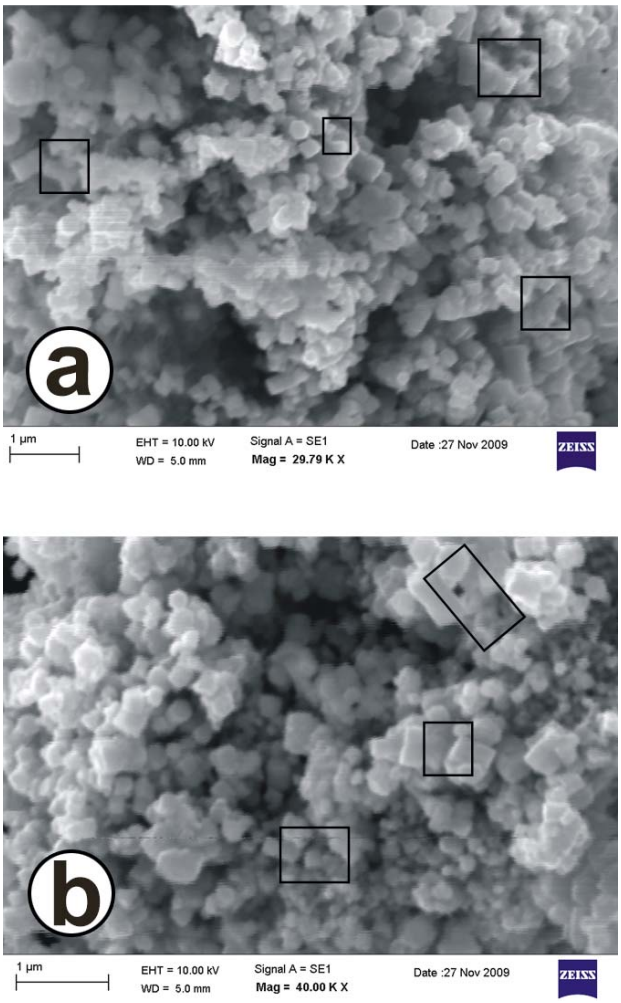

Fig 1. SEM micrographs of (a) prepared ZnO nanoparticles (b) magnified image of (a).

Structural characterization - XRD

Figure 2 shows the XRD patterns of the prepared sample, which indicate that the ZnO phase is of wurtzite structure. The different peaks can be indexed to a hexagonal structure (space group P63mc, JCPDS card no: 36-1451). Compared with the standard diffraction patterns (Table 1), no characteristic peaks from impurities were detected, indicating high purity of the product. Also, the highly intense, sharp peaks indicate that the product is well crystallized.

© The Author 2016. All rights reserved.

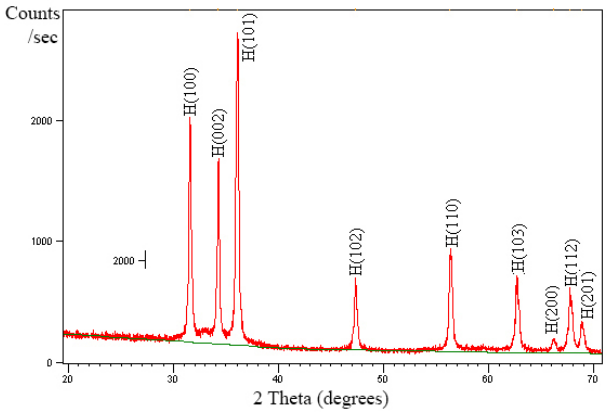

Fig 2. X-ray diffraction pattern of the prepared ZnO nanorods (H-hexagonal)

The lattice parameter of the ZnO nanostructure was calculated using the equation:

$$\frac{1}{d^2} = \frac{4}{3}\left(\frac{1}{a^2}\right) + \frac{1}{c^2}$$

where d is the interplanar distance, and a and c are the lattice parameters ($c/a = \sqrt{8/3}$, for hexagonal structure).

The grain size (D) was calculated by Scherrer's equation [20]:

$$D = \frac{0.9\lambda}{\beta \cos\theta}$$

where λ, β and θ are the X-ray wavelength (0.154056nm), full width at half maximum (FWHM) and Bragg diffraction peak location, respectively.

The grain size and lattice parameters calculated from the most intense peak of the prepared samples were 37.91nm and a=0.3256nm, c=0.5317nm, respectively. The small shift in the value of lattice parameters from that of the bulk value is attributed to the strain in the samples that occurred during the growth process. The strain value was determined using the relation given in Kaczmarek et al. [21]. The value of strain calculated for the most intense (101) plane is 2.1321.

Table 1. Structural parameters of ZnO nanorods.

2θ (deg)		FWHM (deg)	I/I_o	D (nm)	(hkl)	d (Å)	
Observed	JCPDS					Observed	JCPDS
31.567	31.770	0.2204	68.05	37.46	(100)	2.834	2.814
34.255	34.422	0.2204	53.70	37.72	(002)	2.618	2.603
36.058	36.253	0.2204	100	37.91	(101)	2.491	2.476
56.353	56.603	0.3149	28.77	28.66	(110)	1.633	1.625
62.677	62.864	0.2519	22.13	36.93	(103)	1.482	1.477

The growth process of ZnO nanorods can be explained by the initial precipitation of $Zn(OH)_2$. $Zn(OH)_2$, formed during the chemical process, dissolves in water; to a considerable extent, to form Zn^{2+} and OH^- ions. As the concentration of these ions exceeds a critical value, precipitation of ZnO nuclei starts. The chemical reaction proceeds as follows:

$$Zn(OH)_2 \rightarrow Zn^{2+} + 2OH^-$$
$$Zn^{2+} + 2OH^- \rightarrow ZnO + H_2O$$

It has been reported that $Zn(OH)_2$ is more soluble than ZnO. Therefore, the already formed $Zn(OH)_2$ decomposes, continuously producing Zn^{2+} and OH^- ions, which form ZnO nuclei, building blocks for the final products. According to the crystal growth habits of ZnO, ZnO is a polar crystal, where zinc and oxygen atoms are arranged alternately along the c-axis and the top surface is Zn-terminated (0001), while the bottom surface is oxygen-terminated (0001) [22]. Moreover, the growth of ZnO crystals is dependent upon the growth velocities of the different growth planes in ZnO crystals. It has been reported that [22] growth velocity is greater along the (0001) direction of rod-like crystal growth.

OPTICAL CHARACTERIZATION

UV-VIS diffuse reflectance spectra

The diffuse reflectance spectra of the ZnO nanoparticles were recorded as a function of wavelength in the wavelength range 200-800nm, as shown in Figure 3. The average value of reflectance was 75% in the visible range of electromagnetic radiation.

© The Author 2016. All rights reserved.

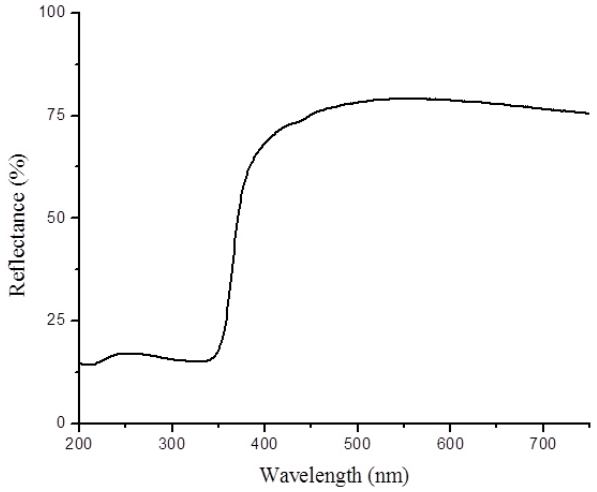

Fig 3. Diffuse reflectance spectra of the prepared ZnO nanoparticles

The band gap of semiconductors is influenced by various factors: temperature, pressure, electric and magnetic fields, impurities, etc. Therefore, band gap is responsive to the structural perfection of the material. The diffuse reflectance, R, is related to the Kubelka – Munk function F(R) by the relation [23]:

$$F(R) = (1-R)^2 / 2R$$

Band gap of ZnO nanoparticles was calculated by plotting $F(R)^2$ vs. hv, as shown in Figure 4. The linear part of the curve was extrapolated to $F(R)^2 = 0$ to get the direct band gap energy. The value of band gap energy thus obtained was 3.42 eV. The increase of band gap from the bulk value (3.37 eV) can be explained on the basis of change in lattice parameter due to the kinetics of the growth process.

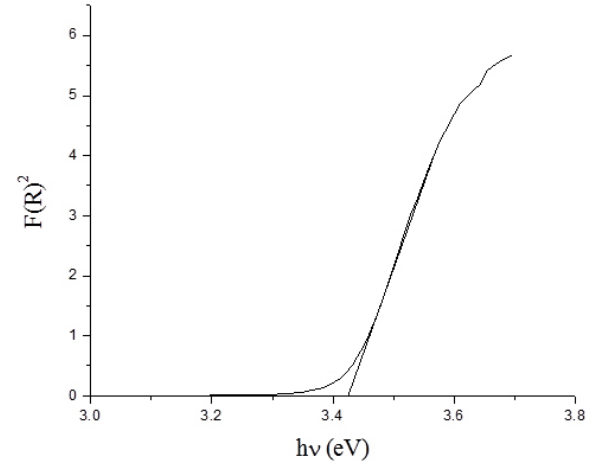

Fig 4. Determination of optical band gap – plot of $F(R)^2$ vs. hv

Photoluminescence spectra

Photoluminescence (PL) properties of ZnO nanorods are some of the most interesting and important properties that have been recently investigated. PL spectra of the prepared sample and samples annealed at 523 K and 673 K are shown in Figure 5.

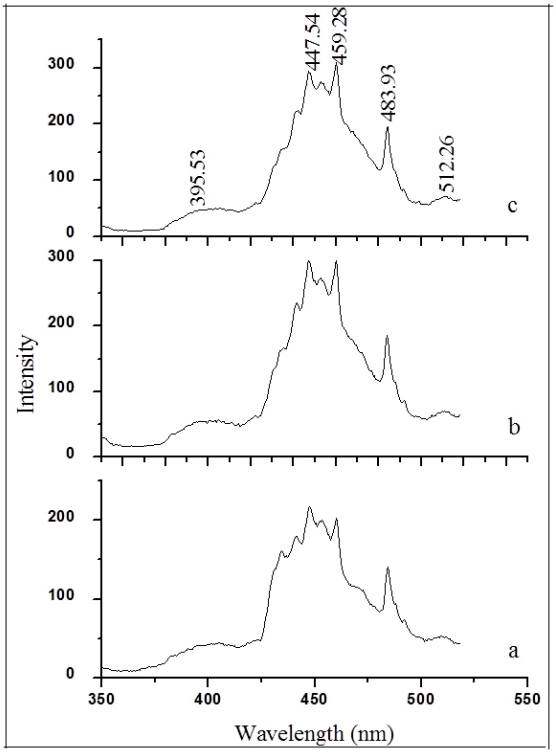

Fig 5. PL spectra of (a) prepared sample and samples calcined at (b) 523 K and (c) 673 K.

Different from the intense UV emission peaks (near-band edge emission) of ZnO nanorods at 385 and 386 nm observed by Guo et al. and Cheng et al. [24,25], a weak broad band from 380 – 410 nm (centered at 395 nm), is observed in our study. In bulk materials, the intensity ratio of near-band edge emission to deep level emission is very low [26]. The broad, near-band edge UV emission may be attributed to the direct recombination of excitons through an exciton-exciton collision process, where one of the excitons radiatively recombines to generate a photon [27]. The strong blue emission observed at 447 and 459 nm (deep level emission) may be related to the intrinsic defects due to O and Zn vacancies or interstitials and their complexes in ZnO materials [27]. The weak broadband located at 512 nm in the visible region is the green band emission, which is attributed to the presence of singly ionized oxygen vacancies [28]. An additional peak at 483

© The AIC 2016. All rights reserved.

nm, which was not previously reported, was also observed in our studies. An increase in emission intensity is observed as calcination temperature is increased to 623 K.

CONCLUSION

ZnO nanorods were prepared by a simple precipitation from an aqueous solution route using zinc nitrate hexahydrate [$Zn(NO_3)_2.6H_2O$] and sodium hydroxide (NaOH). XRD analysis of the nanorods showed that the samples were highly crystalline with a hexagonal wurtzite structure. The optical band gap calculated from the reflectance spectra was 3.37eV. In the PL spectra, weak near-band emissions centered around 395 nm and very intense deep level emissions at 447 and 459 were observed. The intensity of emissions increased with the increase of calcination temperature. One of the implications of this method of preparing nanorods is that this would make a simple, cost-efficient laboratory project in nanomaterials preparation and analysis.

REFERENCES

1. Shalimov A, Paszkowicz W, Grasza K, Skupinski P, Mycielsk A, Bak-Misiuk J. *Phys. Status Solidi*, 2007, (b) 244, 1573-1577.
2. Thomas DG. *J. Phys. Chem. Solids*, 1960, 15, 86-96.
3. Chen Y, Bagnall D, Yao T. *Mater. Sci. Eng.*, 2000, B 75, 190-198.
4. Wang JL. *J. Phys. Condens. Matter*, 2004, 16, R829.
5. Shinde SD, Patil GE, Kajale DD, Ahire DV, Gaikwad VB, Jain GH. *Intl. J. Smart Sensing and Intelligent Systems*, 2012, 5.
6. Wei H, Wu Y, Lun N, Hu C. *Mater. Sci. Eng.*, 2005, A 393, 80-82.
7. Balaguera-Gelves MR, Perales-Perez OJ, Singh SP, Jimenez JA, Aparico-Bolonos JA, Hernandez-Rivera SP. *Mater. Sci. Appln.*, 2013, 4, 29-38.
8. Saaravanan P, Alam S, Mathur GN. *Mater. Lett.*, 2004, 58, 3528-3531.
9. Kamalasanan MN, Chandra S. *Thin Solid Films*, 1996, 288, 112-115.
10. Mueller R, Madler L, Pratsins SE. *Chem. Engg. Sci.*, 2003, 58, 1969-1976.
11. Zhang Y, Dai Y, Huang Y, Zhou C. *J. Univ. Sci. Tech.*, 2004, Beijing 11, 23-29.
12. Li JY, Chen XL, Li H, He M, Qiao ZY. *J. Crys. Growth*, 2001, 233, 5-7.
13. Sue K, Kimura K, Yamamto M, Arai K. *Mater Lett*, 2004, 58, 3350-3352.
14. Xu C, Xu G, Liu Y, Wang GA. *Solid State Commun.*, 2002, 122, 175-179.
15. Hu JQ, Ma XL, Xie ZY, Wong NB, Lee CS, Lee ST. *Chem. Phys. Lett.*, 2001, 344, 97-100.
16. Liu Y, Liu Z, Wang G. *J. Crys. Growth*, 2003, 252, 213-218.
17. Lyu SC, Zhang Z, Ruh H, Lee HJ, Shim HW, Suh EK, Lee CJ. *Chem. Phys. Lett.*, 2002, 363, 134-138.
18. Mali SS, Kim H, Patil PS, Hong CK. *Dalton Trans.*, 2013, 42, 16961-16967.
19. Tang Q, Zhou W, Shen J, Zhang W, Kong L, Qian Y, *Chem. Commun.*, 2004, 712-713.
20. Azaroff LV in *Elements of Crystallography*, McGraw Hill, New York, 1968.
21. Kaczmarek D, Domaradzki J, Wojcieszak D, Wasielewski R, Borkowska A, Prociow EL, Ciszewski A. *Applied Surface Science*, 2008, 254, 4303-4307.
22. Al-Hajry A, Umar A, Hahn YB, Kim DH. *Superlattices and Microstructures*, 2009, 45, 529-534.
23. Kortum G in *Reflectance Spectroscopy*, Springer Verlag, New York.
24. Guo L, Ji YL, Xu HB, Simon P, Wu ZY. *J. Am. Chem. Soc.*, 2002, 124, 14864-14865.
25. Cheng CW, Xu GY, Zhang HQ, Luo Y, Li YY. *Mater. Lett.*, 2008, 52, 3733-3735.
26. Chen Y, Bagnall D, Yao T. *Mater. Sci. Eng.*, 2000, B75, 190–198.
27. Dai L, Chen XL, Wang WJ, Zhou T, Hu BQ. *J. Phys. Condens. Matter*, 2003, 15, 2221.
28. Huang MH, Wu Y, Feick H, Tran N, Weber E, Yang P. *Adv. Mater.*, 2001, 13, 113-116.

© The AIC 2016. All rights reserved.